A BAYESIAN APPROACH FOR THE JOINT ESTIMATION OF THE MULTIFRACTALITY PARAMETER AND INTEGRAL SCALE BASED ON THE WHITTLE APPROXIMATION

S. Combrexelle[1], H. Wendt[1], P. Abry[2], N. Dobigeon[1], S. McLaughlin[3], J.-Y. Tourneret[1]

[1] IRIT - ENSEEIHT, CNRS, University of Toulouse, F-31062 Toulouse, France, `firstname.lastname@enseeiht.fr`

[2] CNRS, Physics Dept., Ecole Normale Supérieure de Lyon, F-69364 Lyon, France, `patrice.abry@ens-lyon.fr`

[3] School of Engineering and Physical Sciences, Heriot-Watt University, Edinburgh, UK, `s.mclaughlin@hw.ac.uk`

ABSTRACT

Multifractal analysis is a powerful standard signal processing tool. Multifractal models are essentially characterized by two parameters, the so-called multifractality parameter c_2 and the integral scale $\mathcal{A}$ (the time scale beyond which multifractal properties vanish). Yet, most applications concentrate on estimating c_2 while estimating $\mathcal{A}$ is mostly overlooked, despite of $\mathcal{A}$ potentially conveying important information. Joint estimation of c_2 and $\mathcal{A}$ is challenging due to the statistical nature of multifractal processes (strong dependence, non-Gaussian), and has barely been considered. The present contribution addresses these limitations and proposes a Bayesian procedure for the joint estimation of $(c_2, \mathcal{A})$. Its originality resides, first, in the construction of a generic multivariate model for the statistics of wavelet leaders for multifractal multiplicative cascade processes, and second, in the use of a suitable Whittle approximation for the likelihood associated with the model. The resulting model enables Bayesian estimators for $(c_2, \mathcal{A})$ to be computed also for large sample size. Performance is assessed numerically for synthetic multifractal processes and illustrated for wind-tunnel turbulence data. The proposed procedure significantly improves estimation of c_2 and yields, for the first time, reliable estimates for $\mathcal{A}$.

Index Terms— Multifractal Analysis, Integral Scale, Wavelet Leaders, Bayesian Estimation, Whittle Likelihood

1. INTRODUCTION

Context. Scale invariance provides practitioners with a powerful concept for real-world data analysis. It has been used in a large variety of applications of very different natures, e.g., biomedical applications (body rhythms [1], infra slow brain activity [2]), hydrodynamic turbulence [3]), geophysics [4], finance [5], Internet traffic [6], to name but a few. Scale invariance implies that the temporal dynamics of data are not driven by any particular scale that could play a privileged role in analysis. Instead, a large continuum of time scales equally contributes to temporal dynamics. From a practical perspective, this translates into power law behaviors of the sample moments of well chosen multi-scale quantities $T_X(a,t)$ (quantities that depend jointly on time t and scale a, such as wavelet coefficients), i.e.

$$S(q,j) \equiv \frac{1}{n_j}\sum_{k=1}^{n_j} |T_X(a,k)|^q \simeq a^{\zeta(q)},\ a_m \leq a \leq a_M. \quad (1)$$

The goal of scale invariance is hence to estimate the *scaling exponents* $\zeta(q)$ that characterize the mechanisms relating scales.

This work was supported by ANR BLANC 2011 AMATIS BS0101102.

S. Combrexelle was supported by the Direction Générale de l'Armement (DGA).

Multifractal analysis consists of a specific instance of scale invariance analysis (cf. e.g., [7]). It notably enables discrimination between two classes of processes commonly used to model scale invariance: self-similar processes, characterized by $\zeta(q) \equiv qH$ and an underlying *additive* structure [8], the fractional Brownian motion (fBm) being the celebrated representative member [9]; multifractal multiplicative cascades (hereafter denoted MMC), characterized by a strictly concave $\zeta(q)$ and an underlying *multiplicative* structure [3]. Deciding which model is preferred by data is of utmost importance in applications as it may significantly modify the understanding and interpretations of the underlying mechanisms producing the data.

The scaling exponents $\zeta(q)$ of MMC can be expanded as a function of q, $\zeta(q) = c_1 q + c_2 q^2/2 + \ldots$, with strictly negative $c_2 < 0$, while $\zeta(q) = qH$ and $c_2 \equiv 0$ for self-similar processes. The discrimination between self-similar processes and MMC can thus be recast into testing $c_2 \equiv 0$ versus $c_2 < 0$ (cf. e.g, [10, 11]) and c_2 is therefore often referred to as the *multifractality* or *intermittency* parameter. The second fundamental difference between self-similar processes and MMC is that the power law relation in (1) theoretically holds for all scales $a > 0$ for self-similar processes, while holds only within a range of scales that is necessary bounded from above, $0 < a \leq \mathcal{A}$, for MMC. This upper bound is commonly referred to as the *integral scale* [3, 12].

While most research concentrate on the estimation of the sole parameter c_2, the integral scale $\mathcal{A}$ has mostly been overlooked. Yet, it conveys fundamental information since it subtly reintroduces a notion of typical (decorrelation) time scale within the scale invariance framework (cf. [13] for a review). This may provide insights into the mechanisms underlying data production. The estimation of the integral scale $\mathcal{A}$ constitutes the core topic of the present contribution.

Related work: Joint estimation of c_2 and $\mathcal{A}$. It is now well understood that the estimation of c_2 (and the detection of deviations of $\zeta(q)$ from a linear behavior in q) should be based on recently proposed refined multi-scale quantities termed *wavelet leaders*, cf., e.g., [7, 10]. The estimation of c_2 essentially relies on linear regressions across scales, motivated by (1) and variations (cf., (2) in Section 2). To improve estimation (notably for small sample size), a generalized moment approach has been proposed, relying strongly on fully parametric models [14] and hence is of limited applicability to real-world data. Alternatively, the use of Bayesian models was proposed but remained mostly restricted to the estimation of the self-similarity parameter for Gaussian processes [15–17]. Only recently, new Bayesian models were proposed for the estimation of c_2, either by considering specific properties of certain processes [18] or by exploiting generic properties of wavelet leaders [19] that are valid for large classes of MMC.

In contrast, the estimation of the integral scale $\mathcal{A}$ has received limited attention. In certain applications, the order of magnitude of the integral scale can be approximately inferred from a priori available physical parameters (typically flow size, average flow speed, …, e.g., for climatology and rainfall analysis [20,21] and for hydrodynamic turbulence [12,22–24]), while this is not possible in most other applications. At the methodological level, an extension of the generalized moment approach to the estimation of the integral scale was proposed in [25] (see also [24]), yet with limited use in applications due to the requirement of fully parametric models.

Contributions. The present work aims at developing a Bayesian model for the joint estimation of the multifractality parameter c_2 and the integral scale $\mathcal{A}$. The procedure generalizes [19], which proposed the first wavelet-leader based Bayesian estimator for the sole parameter c_2, yet assumes $\mathcal{A} \approx n$ and is intractable for sample size larger than $n \sim 10^3$. The main contributions of the present work lie, first, in the generalization of the statistical model proposed in [19] to $\mathcal{A} \leq n$, enabling the formulation of a joint estimator for $(c_2, \mathcal{A})$, and second, the use of a suitable Whittle likelihood in the Bayesian procedure [26–29], enabling their use for large sample sizes.

We first propose a semi-parametric model for the statistics of the log-wavelet leaders of MMC, motivated by the asymptotic covariance of the logarithm of multiscale quantities associated with these processes (c.f. [3]). The model is generically valid for this class of processes, for all values of $\mathcal{A}$. It imposes minimal model assumptions on data (essentially, (2) below) and involves few parameters (effectively, c_2 and $\mathcal{A}$, cf. Section 3.1). From this model, a Bayesian estimation procedure for $(c_2, \mathcal{A})$ is developed by assigning an appropriate prior distribution to the parameters, reflecting the constraints inherent to the multifractal model. To explore the resulting posterior distribution and generate samples used to approximate the Bayesian estimators, a suitable MCMC random-walk Metropolis-Hastings sampling scheme is devised (cf. Section 3).

The direct evaluation of the likelihood in the MCMC scheme would require, at each iteration, the inversion of a dense matrix of essentially the order of the sample size n, which is prohibitive both numerically and computationally for large n. To overcome this difficulty, we propose to approximate the exact likelihood induced by the multifractal model by an appropriate Whittle likelihood (cf. Section 4). The resulting algorithm for the joint estimation of c_2 and $\mathcal{A}$ is effective for both small and large sample sizes. Its performance is assessed by means of Monte Carlo simulations, showing the clear benefits of the Bayesian estimator over linear regressions for the estimation of c_2, and its effectiveness for the reliable estimation of the integral scale $\mathcal{A}$ (cf. Section 5). Finally, we illustrate the potential of the proposed Bayesian procedure for the analysis of a high-quality real-world data set of wind-tunnel turbulence.

2. MULTIFRACTAL ANALYSIS

Discrete wavelet transform. A mother wavelet $\psi_0(t)$ is a reference pattern with narrow supports in both time and frequency domains. It is characterized by its number of vanishing moments $N_\psi \geq 1$ ($\forall k = 0, 1, \ldots, N_\psi - 1$, $\int_{\mathbb{R}} t^k \psi_0(t) dt \equiv 0$ and $\int_{\mathbb{R}} t^{N_\psi} \psi_0(t) dt \neq 0$). Also, it is chosen such that the collection $\{\psi_{j,k}(t) \equiv 2^{-j/2} \psi_0(2^{-j}t - k), j \in \mathcal{N}, k \in \mathcal{N}\}$ forms a basis of $L^2(\mathbb{R})$. The discrete wavelet transform (DWT) coefficients of X are defined as $d_X(j,k) = \langle X, \psi_{j,k} \rangle$, cf., e.g., [30] for further details.

Wavelet leaders. Let denote $\lambda_{j,k} = [k2^j, (k+1)2^j)$ the dyadic interval of size 2^j and $3\lambda_{j,k}$ the union of $\lambda_{j,k}$ with its 2 neighbors. The wavelet leaders are defined as the largest wavelet coefficient in the neighborhood $3\lambda_{j,k}$ over all finer scales, $\boldsymbol{\ell}(j,k) := \sup_{\lambda' \subset 3\lambda_{j,k}} |d_X(\lambda')|$ [7,31].

Multifractal formalism. The wavelet leader scaling function is defined as $\zeta(q) = \liminf_{j \to -\infty} \left[\ln S(j,q) / \ln 2^j \right]$ where $S(j,q) = 2^j \sum_k \boldsymbol{\ell}(j,k)^q$ are the empirical moments of order q of the wavelet leaders of X at scale j. The function $\zeta(q)$ is intimately tied to the multifractal spectrum $D(h)$ via a Legendre transform, $D(h) \leq \mathcal{L}(h) := \inf_{q \in \mathbb{R}} [1 + qh - \zeta(q)]$. It can be shown that this inequality is strict for large classes of multifractal processes. The Legendre spectrum $\mathcal{L}(h)$ is thus practically often confounded with the theoretical spectrum $D(h)$, see [10,31].

Log-cumulant expansion. It is often advantageous in applications to work with the leading order coefficients of the polynomial expansion $\zeta(q) = \sum_{m \geq 1} c_m q^m / m!$ of the scaling function. This expansion directly translates to $D(h)$, see [31]. In particular, the first log-cumulant c_1 is identical to the position of the mode of $D(h)$ (i.e., the average smoothness), and the second log-cumulant c_2 is directly related to its width (i.e., the degree of regularity fluctuations). The seminal work [32] shows that the c_m are directly related to the cumulants of order m of the log-wavelet leaders, $\mathrm{Cum}_m[\ln \boldsymbol{\ell}(j,k)] = c_m^0 + c_m \ln 2^j$ and specifically,

$$C_2(j) \equiv \mathrm{Var}\left[\ln \boldsymbol{\ell}(j,k)\right] = c_2^0 + c_2 \ln 2^j. \quad (2)$$

The parameter c_2 can thus be estimated by linear regression of the sample variance (denoted $\widehat{\mathrm{Var}}$) of $\ln \boldsymbol{\ell}(j,\cdot)$ against scale $j \in [j_1, j_2]$

$$\hat{c}_2 = \frac{1}{\ln 2} \sum_{j=j_1}^{j_2} w_j \widehat{\mathrm{Var}}[\ln \boldsymbol{\ell}(j,k)] \quad (3)$$

where w_j are suitable regression weights, see [6,10] for details.

3. BAYESIAN ESTIMATION

3.1. Model for the multivariate statistics of log-wavelet leaders

Let $l(j,k) = \ln \boldsymbol{\ell}(j,k)$ denote the log-wavelet leaders. We propose a model for the multivariate statistics of $l(j,\cdot)$ of MMC that generalizes the model in [19] to MMC with integral scale $\mathcal{A} \leq n$.

Marginal distributions. It has been shown in [19] that the marginal distribution of $l(j,\cdot)$ of MMC can be approximated by a Gaussian distribution. This is illustrated in Fig. 1 (top row) for different integral scale values for the process described in Section 5.

Covariance. The numerical studies reported in [19] suggest that the covariance of the logarithm of wavelet leaders of MMC processes at fixed scale j, $\Sigma_j(\Delta k) := \mathrm{Cov}[l(j,k), l(j,k+\Delta k)]$, is characterized by a logarithmic decay controlled by the parameter c_2

$$\Sigma_j(\Delta k) \approx \eta + c_2(\ln \Delta k + \ln 2^j) =: \gamma_j^{(1)}(\Delta r; c_2, \eta) \quad (4)$$

for $3 \leq \Delta k \leq n_j \frac{\mathcal{A}}{n}$, where $n_j \approx \lfloor n/2^j \rfloor$ denotes the number of wavelet leaders at scale j (see also [33] for results obtained for log-wavelet coefficients of 1D random wavelet cascades). Second, the theoretical variance of the log-wavelet leaders is given by $C_2(j) = C_2(j; c_2, c_2^0)$ defined in (2). Finally, we propose to model the short-term covariance as a logarithmic decay from $C_2(j; c_2, c_2^0)$ at $\Delta k = 0$ to $\gamma_j^{(1)}(\Delta r; c_2, \eta)$ at $\Delta k = 3$,

$$\gamma_j^{(0)}(\Delta k; c_2, c_2^0, \eta) := C_2(j; c_2, c_2^0) + \Big(\ln(\Delta k + 1)/\ln 4\Big)\Big(\gamma_j^{(1)}(3; c_2, \eta) - C_2(j; c_2, c_2^0)\Big). \quad (5)$$

By combining (2), (4) and (5), we obtain the following model for the covariance of log-wavelet leaders, parametrized by $\boldsymbol{\theta} = [c_2, c_2^0, \eta]^T$

$$\gamma_j(\Delta k; \boldsymbol{\theta}) = \begin{cases} C_2(j; c_2, c_2^0) & \Delta k = 0 \\ \gamma_j^{(0)}(\Delta k; c_2, c_2^0, \eta) & 0 < \Delta k \leq 3 \\ \max[0, \gamma_j^{(1)}(\Delta k; c_2, \eta)] & 3 < \Delta k \leq n_j. \end{cases} \quad (6)$$

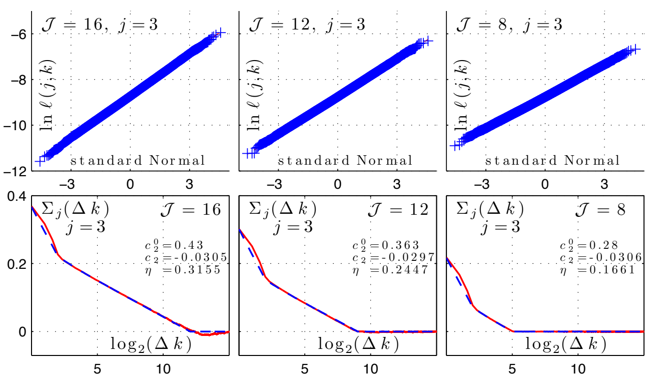

Fig. 1: Top row: quantile-quantile plots of $\ln \boldsymbol{\ell}(j=3,k)$ against standard normal. Bottom row: Empirical covariances of $\ln \boldsymbol{\ell}(j=3,k)$ (red solid) and model (6) (blue dashed). Left to right: $\mathcal{J}=\{16,12,8\}$, respectively. Results obtained for MRW as in Section 5.

Here, the restriction of $\gamma_j^{(1)}$ to positive values encodes the range of validity, $3 \leq \Delta k \leq n_j \frac{\mathcal{A}}{n}$, of (4). The model is illustrated in Fig. 1 (bottom row).

Integral scale. The integral scale $\mathcal{A}$ corresponds to the typical correlation length of the data. It is therefore directly related to the pair (η, c_2) in (4) through the equation

$$\mathcal{J}=\mathcal{J}(\eta, c_2) := \log_2(\mathcal{A}) = -\eta/(c_2 \ln(2)).$$

Note that η was not a model parameter in [19] but an a priori fixed heuristic constant, unrelated to the integral scale $\mathcal{A}$ of the data.

3.2. Bayesian model

Let $\boldsymbol{l}_j$ denote the vector of the n_j centered log-leaders $l(j,k) - \bar{l}_X(j,.)$ and $\boldsymbol{\Gamma}_j(\boldsymbol{\theta})$ the corresponding $n_j \times n_j$ covariance matrix with entries given by the parametric covariance (6), respectively.

Likelihood. Due to the Gaussian properties of the log-wavelet leaders, the likelihood of the vector $\mathcal{L}=[\boldsymbol{l}_{j_1}^T, ..., \boldsymbol{l}_{j_2}^T]^T$ is given by $f(\mathcal{L}|\boldsymbol{\theta}) = \prod_{j=j_1}^{j_2} L(\boldsymbol{l}_j|\boldsymbol{\theta})$ with

$$L(\boldsymbol{l}_j|\boldsymbol{\theta}) := \left((2\pi)^{n_j} \det \boldsymbol{\Gamma}_j(\boldsymbol{\theta})\right)^{-\frac{1}{2}} \exp\left(-\frac{1}{2}\boldsymbol{l}_j^T \boldsymbol{\Gamma}_j(\boldsymbol{\theta})^{-1}\boldsymbol{l}_j\right). \quad (7)$$

Prior distribution. The parameter vector $\boldsymbol{\theta}=[c_2, c_2^0, \eta]^T$ must be chosen such that the variances of $l(j,k)$ are positive, i.e., $C_2(j) \geq 0$. We define the admissible set $\mathcal{I}=(\mathcal{I}^+ \cup \mathcal{I}^-) \cap \mathcal{I}^m$, where $\mathcal{I}^- = \{\boldsymbol{\theta} \in \mathbb{R}^3 | c_2 < 0 \text{ and } c_2^0 + c_2\ j_2 \ln 2 > 0\}$, $\mathcal{I}^+ = \{\boldsymbol{\theta} \in \mathbb{R}^3 | c_2 > 0 \text{ and } c_2^0 + c_2\ j_1 \ln 2 > 0\}$, $\mathcal{I}^m = \{\boldsymbol{\theta} \in \mathbb{R}^3 || c_2^0| < c_2^{0,m}, |c_2| < c_2^m, |\eta| < \eta^m\}$ and $c_2^m, c_2^{0,m}, \eta^m$ are the largest admissible values for c_2, c_2^0 and η. Without additional prior information regarding $\boldsymbol{\theta}$, a uniform prior distribution on the set $\mathcal{I}$ is assigned to $\boldsymbol{\theta}$, i.e., $\mathcal{P}(\boldsymbol{\theta}) = U_{\mathcal{I}}(\boldsymbol{\theta}) \propto \mathbf{1}_{\mathcal{I}}(\boldsymbol{\theta})$, where $\mathbf{1}_{\mathcal{I}}$ is the indicator function of $\mathcal{I}$.

Posterior distribution and Bayesian estimators. The posterior distribution of $\boldsymbol{\theta}$ is obtained from the Bayes rule

$$f(\boldsymbol{\theta}|\mathcal{L}) \propto f(\mathcal{L}|\boldsymbol{\theta})\, \mathcal{P}(\boldsymbol{\theta}) \quad (8)$$

and can be used to define the maximum a posteriori (MAP) and minimum mean squared error (MMSE) estimators in (9) below.

3.3. Gibbs sampler

The following Gibbs sampler enables the generation of samples $\{\boldsymbol{\theta}^{(t)}\}_1^{N_{mc}}$ that are asymptotically distributed according to the posterior distribution (8). The Gibbs sampling strategy consists of successively sampling according to the conditional distributions associated with $f(\boldsymbol{\theta}|\mathcal{L})$. To sample according to the conditional distributions, a Metropolis-within-Gibbs procedure is used, defined by random walks with Gaussian instrumental distributions. More precisely, at iteration $\#t$, the three following moves are considered.

Sampling according to $f(c_2^{(t)}|c_2^{0,(t-1)}, \eta^{(t-1)}, \mathcal{L})$. A candidate c_2^* is generated according to the proposal distribution $q_{c_2}(c_2^*|\mathcal{L}) = \mathcal{N}(c_2^{(t-1)}, \sigma_{c_2}^2)$. It is accepted ($c_2^{(t)} = c_2^*$) or rejected ($c_2^{(t)} = c_2^{(t-1)}$) according to the Metropolis-Hastings ratio r_{c_2}.

Sampling according to $f(c_2^{0,(t)}|c_2^{(t)}, \eta^{(t-1)}, \mathcal{L})$. A candidate $c_2^{0,*}$ is generated according to the proposal distribution $q_{c_2^0}(c_2^{0,*}|\mathcal{L}) = \mathcal{N}(c_2^{0,(t-1)}, \sigma_{c_2^0}^2)$ and accepted ($c_2^{0,(t)} = c_2^{0,*}$) or rejected ($c_2^{0,(t)} = c_2^{0,(t-1)}$) according to the Metropolis-Hastings ratio $r_{c_2^0}$.

Sampling according to $f(\eta^{(t)}|c_2^{(t)}, c_2^{0,(t)}, \mathcal{L})$. A candidate η^* is generated according to the proposal distribution $q_\eta(\eta^*|\mathcal{L}) = \mathcal{N}(\eta^{(t-1)}, \sigma_\eta^2)$. It is accepted ($\eta^{(t)} = \eta^*$) or rejected ($\eta^{(t)} = \eta^{(t-1)}$) according to the Metropolis-Hastings ratio r_η.

The Metropolis-Hastings acceptance ratios are defined by $r_\theta = \frac{f(\boldsymbol{\theta}^*|\mathcal{L})}{f(\boldsymbol{\theta}^{(t-1)}|\mathcal{L})} \frac{q_\theta(\theta^{(t-1)}|\mathcal{L})}{q_\theta(\theta^*|\mathcal{L})}$. The variances $\sigma_{(\cdot)}^2$ of the instrumental distributions are adjusted to ensure acceptance ratios belonging to the interval $[0.4, 0.6]$. For details about MCMC methods, see, e.g., [34].

Bayesian estimators. After a burn-in period of N_{bi} samples, the Gibbs sampler generates $N_B = N_{mc} - N_{bi}$ samples $\{\boldsymbol{\theta}^{(t)}\}_{N_{bi}+1}^{N_{mc}}$ that are distributed according to (8) and used to approximate the Bayesian estimators

$$\hat{\boldsymbol{\theta}}^{MMSE} \approx \frac{1}{N_B}\sum_{t=N_{bi}+1}^{N_{mc}} \boldsymbol{\theta}^{(t)}, \ \hat{\boldsymbol{\theta}}^{MAP} \approx \underset{t>N_{bi}}{\operatorname{argmax}}\, f(\boldsymbol{\theta}^{(t)}|\mathcal{L}). \quad (9)$$

4. WHITTLE APPROXIMATION

The Gibbs sampler requires inversion of the dense $n_j \times n_j$ matrices $\boldsymbol{\Gamma}_j(\boldsymbol{\theta})$ in each sampling step. For large sample size, this is practically intractable both for practical (computation time) and numerical (growing condition number of $\boldsymbol{\Gamma}_j(\boldsymbol{\theta})$) reasons. To handle large sample sizes, we replace the exact likelihood (7) with the approximate Whittle likelihood [26, 27]. Up to an additive constant, the Whittle approximation for the negative log-likelihood is given by

$$-\ln L(\boldsymbol{l}_j|\boldsymbol{\theta}) \approx \mathcal{W}(\boldsymbol{l}_j|\boldsymbol{\theta}) := \frac{1}{2}\sum_{\omega} \ln \vartheta_j(\omega|\boldsymbol{\theta}) + \frac{\Pi_j(\omega)}{n_j \vartheta_j(\omega|\boldsymbol{\theta})} \quad (10)$$

where $\Pi_j(\omega) := |\sum_{k=1}^{n_j} l(j,k)\exp(\mathrm{i}\omega k)|^2$ is the periodogram of $\{l(j,k)\}_{k\in P_j}$ and $\vartheta_j(\omega|\boldsymbol{\theta}) = |\sum_{k=1}^{n_j} \gamma_j(\Delta k; \boldsymbol{\theta})\exp(\mathrm{i}\omega k)|$ is the Fourier transform of the covariance function (6).

The Whittle likelihood that replaces (7) in (8) is, up to a multiplicative constant, given by

$$f(\mathcal{L} \mid \boldsymbol{\theta}) \approx f_{\mathcal{W}}(\mathcal{L} \mid \boldsymbol{\theta}) := \exp\left(-\sum_{j=j_1}^{j_2} \mathcal{W}(\boldsymbol{l}_j, \boldsymbol{\theta})\right). \quad (11)$$

5. RESULTS

We quantify the estimation performance of the proposed procedure by applying it to a large number R of independent realizations of a synthetic multifractal process, the multifractal random walk (MRW), with different prescribed integral scale values. MRW is chosen here as a prominent member of the class of multifractal multiplicative cascade based processes. MRW is a non Gaussian process with stationary increments. Its multifractal properties mimic those of the

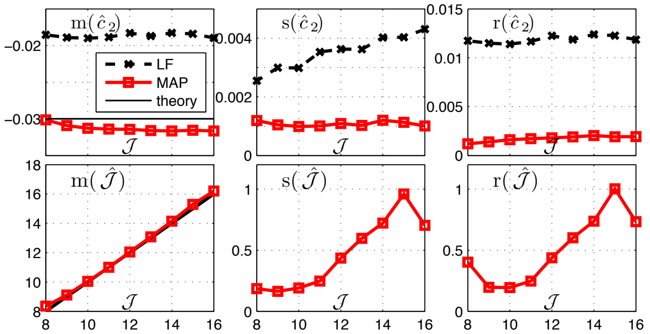

Fig. 2: Estimation of c_2 (top row) and $\mathcal{J} = \log_2(\mathcal{A})$ (bottom row) as a function of the integral scale $\mathcal{J} = \log_2(\mathcal{A})$; average (left column), standard deviation (center column) and RMSE (right column).

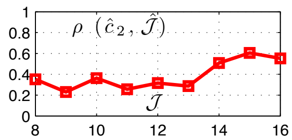

Fig. 3: Correlation coefficient of $\hat{c}_2$ and $\widehat{\mathcal{J}}$ as a function of $\mathcal{J}$.

celebrated Mandelbrot's multiplicative log-normal cascades. Equivalent results are obtained for other multiplicative cascade based processes and are not reported here for space reasons. MRW has been introduced in [35] as $X(k) = \sum_{k=1}^{n} G_H(k) e^{\omega(k)}$ where $G_H(k)$ are the increments of a fractional Brownian motion with parameter H, and ω is a Gaussian process that is independent of G_H and has non trivial covariance $\mathrm{Cov}[\omega(k_1), \omega(k_2)] = -c_2 \ln\left(\frac{\mathcal{A}}{|k_1-k_2|+1}\right)$ when $|k_1 - k_2| < \mathcal{A}$ and 0 otherwise. MRW has scaling properties as in (1) for $q \in \left[-\sqrt{\frac{2}{-c_2}}, \sqrt{\frac{2}{-c_2}}\right]$, with $\zeta(q) = (H - c_2)q + c_2 q^2/2$.

Numerical simulation. The process parameters are set to $H = 0.72$, $c_2 = -0.03$ and $\mathcal{J} = \log_2(\mathcal{A}) \in \{8, \ldots, 16\}$. We use a Daubechies' wavelet with $N_\psi = 2$ vanishing moments and the range of scales $[j_1, j_2] = [3, 6]$ for estimation (j_2 is fixed to the scaling range for $\mathcal{J} = 8$ and could be chosen larger for larger $\mathcal{J}$). We use sample a size $n = 2^{18}$, and $N_{bi} = 3000$, $N_{mc} = 4000$ in the Gibbs sampler. Estimation performance is quantified via the average, the standard deviation and the root square minimum error (RMSE) of the estimates of $\theta \in \{c_2, \mathcal{J}\}$ over $R = 100$ realizations, defined as $\mathrm{m}(\hat{\theta}) = \widehat{\mathbb{E}}[\hat{\theta}]$, $\mathrm{s}(\hat{\theta}) = \sqrt{\widehat{\mathrm{Var}}[\hat{\theta}]}$, $\mathrm{r}(\hat{\theta}) = \sqrt{(m(\hat{\theta}) - \theta)^2 + s(\hat{\theta})^2}$.

Estimation of multifractality parameter c_2. We first compare the linear fit estimator (3) for c_2, denoted LF, with the proposed joint MAP estimator for $(c_2, \mathcal{J})$, denoted MAP; results for the MMSE estimators are similar to MAP and not reproduced here. Results are reported in Fig. 2 (top row), as a function of integral scale $\mathcal{J}$. They indicate that the Bayesian estimator yields excellent estimates for c_2, of remarkably better quality than LF: notably, MAP has significantly smaller standard deviations and bias, resulting in RMSE values that are only one quarter of those of LF (at the price of increased computational cost of $\sim$ 1min for MAP versus $\ll$ 1s for LF).

Estimation of Integral Scale $\mathcal{J}$. Results for the estimation of the integral scale $\mathcal{J}$ obtained by the proposed procedure are reported in Fig. 2 (bottom row; note that LF can not provide estimates of $\mathcal{J}$). They clearly indicate that the proposed procedure is effective and yields consistent estimates of $\mathcal{J}$ for the entire range from very small ($\mathcal{J} = 8$) to large ($\mathcal{J} = 16$) integral scales (hence, correlation length) considered here. In particular, the bias is found to be significantly below standard deviations, and RMSE values are below 10% of the value of $\mathcal{J}$. Estimation performance decreases with increasing $\mathcal{J}$ due to the increasing correlation length of $\sim 2^{\mathcal{J}}$ samples: RMSE values rise from 2% ($\mathcal{J} = 9$) to 6% ($\mathcal{J} = 15$) of the value of $\mathcal{J}$.

Correlation between c_2 and $\mathcal{J}$. Fig. 3 plots the sample correlation coefficient $\rho(\hat{c}_2, \widehat{\mathcal{J}})$ of the estimates of $(c_2, \mathcal{J})$. For large values of $\mathcal{J}$, c_2 and $\mathcal{J}$ show relatively strong correlation. For smaller values of $\mathcal{J}$, $\rho(\hat{c}_2, \widehat{\mathcal{J}})$ decreases since the variances $C_2(j)$ (controlled by c_2 only) become more dominant over the covariance term $\gamma_j^{(1)}(\Delta k; c_2, \eta)$ (jointly controlled by c_2 and $\mathcal{J}$) in (6) (cf. Fig. 1).

Application to Turbulence data. We illustrate the proposed procedure for a large wind-tunnel turbulence data set consisting of high sampling rate longitudinal Eulerian velocity signals, measured with hot-wire anemometry techniques. The dataset, made available to us by Y. Gagne [23], consists of $R = 24$ independent runs of $n = 2^{20}$ samples each, with (Taylor scale based) Reynolds number $\mathcal{R}_\lambda \approx 2000$, integral scale $\mathcal{A} = 2^{13}$, and Taylor scale 2^4. Estimation parameters are set as in [10] (i.e., $[j_1, j_2] = [6, 10]$ and $N_\psi = 3$).

Results are reported in Fig. 4 (c_2 (left) and $\mathcal{J} = \log_2 \mathcal{A}$ (right)) for each individual run and indicate that the proposed procedure yields highly consistent estimates for the different runs, both for c_2 and $\mathcal{J}$. The averages (standard deviations) of the estimates are found to be -0.016 (0.001) for c_2 and 11.78 (0.31) for $\mathcal{J}$, respectively. In view of the above reported results for synthetic data, estimates for $\mathcal{J}$ are within one standard deviation and hence in agreement with the value $\mathcal{J} = 13$ inferred based on Taylor scale in [23].

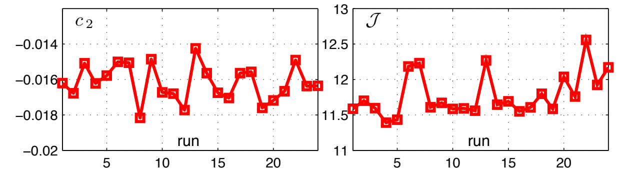

Fig. 4: Joint Bayesian estimation of c_2 (left) and integral scale $\mathcal{J} = \log_2(\mathcal{A})$ (right) for wind-tunnel turbulence data as a function of runs.

6. CONCLUSION

To the best of our knowledge, this paper studied the first Bayesian procedure for the joint estimation of the multifractality parameterc_2 and (log-) integral scale $\mathcal{J}$ that is operational and can be applied to real-world data. It relies on a novel generic semiparametric model for the statistics of the logarithm of wavelet leaders of multiplicative cascade based multifractal processes. A Gibbs sampler is designed to produce samples according to the joint posterior distribution of the multifractal parameter vector, incorporating the multifractal model constraints, which are used to approximate the Bayesian estimators. Computational efficiency of the procedure and applicability to large sample sizes are made possible by using the approximate Whittle likelihood in the sampler. The procedure enables reliable estimation of the integral scale $\mathcal{J}$, previously barely achieved. It significantly improves estimation for the multifractality parameter c_2 over standard linear regression based estimators, reducing standard deviations and RMSE values to 25% of those of linear fit based estimation (at the price of increased computational cost). The procedure is currently being used in the study of 24 hours long heart rate variability time series. Future work will include the extension of the proposed procedure to 2D images and the development of a relevant statistical framework for the multifractal analysis of multivariate time series.

MATLAB codes implementing the proposed procedure, written by the authors, are publicly available at http://www.irit.fr/~Herwig.Wendt/.

7. REFERENCES

[1] A. L. Goldberger, L. A. Amaral, J. M. Hausdorff, P. Ch. Ivanov, C. K. Peng, and H. E. Stanley, "Fractal dynamics in physiology: alterations with disease and aging," *Proc. Natl. Acad. Sci. USA*, vol. 99, no. Suppl 1, pp. 2466–2472, 2002.

[2] P. Ciuciu, G. Varoquaux, P. Abry, S. Sadaghiani, and A. Kleinschmidt, "Scale-free and multifractal dynamic properties of fMRI signals during rest and task," *Frontiers in Physiology*, vol. 3, no. 186, June 2012.

[3] B.B. Mandelbrot, "Intermittent turbulence in self-similar cascades: divergence of high moments and dimension of the carrier," *J. Fluid Mech.*, vol. 62, pp. 331–358, 1974.

[4] E. Foufoula-Georgiou and P. Kumar, Eds., *Wavelets in Geophysics*, Academic Press, San Diego, 1994.

[5] B.B. Mandelbrot, *Fractals and scaling in finance*, Selected Works of Benoit B. Mandelbrot. Springer-Verlag, New York, 1997, Discontinuity, concentration, risk, Selecta Volume E, With a foreword by R. E. Gomory.

[6] P. Abry, P. Flandrin, M. S. Taqqu, and D. Veitch, "Wavelets for the analysis, estimation and synthesis of scaling data," in *Self-Similar Network Traffic and Performance Evaluation*, K. Park and W. Willinger, Eds., pp. 39–88. Wiley, 2000.

[7] S. Jaffard, "Wavelet techniques in multifractal analysis," in *Fractal Geometry and Applications: A Jubilee of Benoît Mandelbrot*, M. Lapidus and M. van Frankenhuijsen, Eds. 2004, vol. 72(2), pp. 91–152, AMS.

[8] G. Samorodnitsky and M. Taqqu, *Stable non-Gaussian random processes*, Chapman and Hall, New York ISBN 0-412-05171-0, 1994.

[9] B.B. Mandelbrot and J.W. van Ness, "Fractional Brownian motion, fractional noises and applications," *SIAM Review*, vol. 10, pp. 422–437, 1968.

[10] H. Wendt, P. Abry, and S. Jaffard, "Bootstrap for empirical multifractal analysis," *IEEE Signal Processing Mag.*, vol. 24, no. 4, pp. 38–48, 2007.

[11] H. Wendt, S. Jaffard, and P. Abry, "Multifractal analysis of self-similar processes," in *Proc. IEEE Workshop Statistical Signal Processing (SSP)*, Ann Arbor, MI, USA, 2012.

[12] U. Frisch, *Turbulence, the Legacy of A. N. Kolmogorov*, Cambridge University Press, 1995.

[13] L. Chevillard, B. Castaing, A. Arneodo, E. Lévêque, J.-F. Pinton, and S. G. Roux, "A phenomenological theory of Eulerian and Lagrangian velocity fluctuations in turbulent flows," *Comptes Rendus Physique*, vol. 13, no. 9, pp. 899–928, 2012.

[14] T. Lux, "Higher dimensional multifractal processes: A GMM approach," *J. Business & Economic Stat.*, vol. 26, pp. 194–210, 2007.

[15] T. T. Lundhal, W. J. Ohley, S. M. Kay, and R. Siert, "Fractional brownian motion: an ML estimator and its application to image texture," *IEEE Trans. on Medical Imaging*, vol. MI-5, no. 3, pp. 152–161, sep 1986.

[16] G.W. Wornell and A. V. Oppenheim, "Estimation of fractal signals from noisy measurements using wavelets," *IEEE Trans. on Signal Processing*, vol. 40, no. 3, pp. 611–623, March 1992.

[17] J. Beran, *Statistics for Long-Memory Processes*, Chapman & Hall, 1994.

[18] O. Løvsletten and M. Rypdal, "Approximated maximum likelihood estimation in multifractal random walks," *Phys. Rev. E*, vol. 85, pp. 046705, 2012.

[19] H. Wendt, N. Dobigeon, J.-Y. Tourneret, and P. Abry, "Bayesian estimation for the multifractality parameter," in *Proc. IEEE Int. Conf. Acoust., Speech, and Signal Process. (ICASSP)*, May 2013.

[20] S. Lovejoy and D. Schertzer, *The weather and climate: emergent laws and multifractal cascades*, Cambridge University Press, 2013.

[21] A. Davis, A. Marshak, W. Wiscombe, and R. Cahalan, "Multifractal characterizations of nonstationarity and intermittency in geophysical fields: Observed, retrieved, or simulated," *Journal of Geophysical Research: Atmospheres (1984–2012)*, vol. 99, no. D4, pp. 8055–8072, 1994.

[22] G. I. Taylor, "Statistical theory of turbulence," *Proceedings of the Royal Society of London. Series A, Mathematical and Physical Sciences*, vol. 151, no. 873, pp. 421–444, 1935.

[23] H. Kahalerras, Y. Malecot, Y. Gagne, and B. Castaing, "Intermittency and Reynolds number," *Physics of Fluids*, vol. 10, no. 4, pp. 910–921, 1998.

[24] E. Bacry, A. Kozhemyak, and J.-F. Muzy, "Continuous cascade models for asset returns," *J. Economic Dynamics and Control*, vol. 32, no. 1, pp. 156–199, 2008.

[25] T. Lux, "The Markov-switching multifractal model of asset returns," *J. Business & Economic Stat.*, vol. 26, no. 2, pp. 194–210, 2008.

[26] P. Whittle, "Estimation and information in stationary time series," *Arkiv för matematik*, vol. 2, no. 5, pp. 423–434, 1953.

[27] M. B. Priestley, *Spectral analysis and time series*, Academic press, 1981.

[28] C. Velasco and P.M. Robinson, "Whittle pseudo-maximum likelihood estimation for nonstationary time series," *J. Am. Statist. Assoc.*, vol. 95, no. 452, pp. 1229–1243, 2000.

[29] K. Shimotsu and P. C. B. Phillips, "Exact local Whittle estimation of fractional integration," *Ann. Stat.*, vol. 33, no. 4, pp. 1890–1933, 2005.

[30] S. Mallat, *A Wavelet Tour of Signal Processing*, Academic Press, San Diego, CA, 1998.

[31] S. Jaffard, P. Abry, and H. Wendt, "Irregularities and scaling in signal and image processing: Multifractal analysis," in *Benoit Mandelbrot: A Life in Many Dimensions*, Michael Frame, Ed. World scientific publishing, 2015.

[32] B. Castaing, Y. Gagne, and M. Marchand, "Log-similarity for turbulent flows," *Physica D*, vol. 68, no. 3-4, pp. 387–400, 1993.

[33] A. Arneodo, E. Bacry, and J.-F. Muzy, "Random cascades on wavelet dyadic trees," *J. Math. Phys.*, vol. 39, no. 8, pp. 4142–4164, 1998.

[34] C. P. Robert and G. Casella, *Monte Carlo Statistical Methods*, Springer, New York, NY, USA, 2 edition, 2004.

[35] E. Bacry, J. Delour, and J.-F. Muzy, "Multifractal random walk," *Phys. Rev. E*, vol. 64: 026103, 2001.